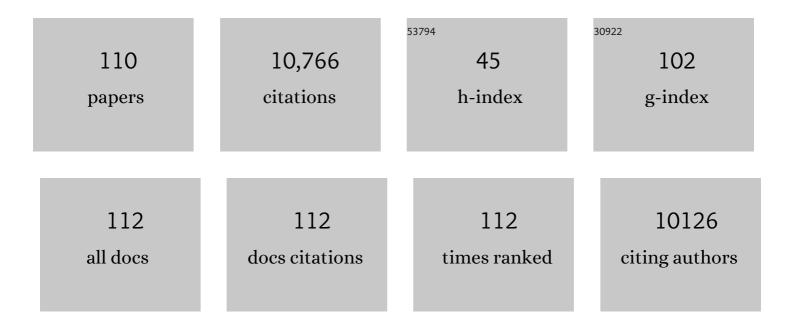
List of Publications by Year in descending order

Source: https://exaly.com/author-pdf/4070048/publications.pdf Version: 2024-02-01



<u> 7наони Млас</u>

#	Article	IF	CITATIONS
1	Semiconductor heterojunction photocatalysts: design, construction, and photocatalytic performances. Chemical Society Reviews, 2014, 43, 5234.	38.1	3,257
2	Effects of chloride ion on degradation of Acid Orange 7 by sulfate radical-based advanced oxidation process: Implications for formation of chlorinated aromatic compounds. Journal of Hazardous Materials, 2011, 196, 173-179.	12.4	502
3	Fe Co3â^O4 nanocages derived from nanoscale metal–organic frameworks for removal of bisphenol A by activation of peroxymonosulfate. Applied Catalysis B: Environmental, 2016, 181, 788-799.	20.2	388
4	Uncertainty and misinterpretation over identification, quantification and transformation of reactive species generated in catalytic oxidation processes: A review. Journal of Hazardous Materials, 2021, 408, 124436.	12.4	297
5	Probing paramagnetic species in titania-based heterogeneous photocatalysis by electron spin resonance (ESR) spectroscopy—A mini review. Chemical Engineering Journal, 2011, 170, 353-362.	12.7	280
6	Photocatalytic degradation of tetracycline antibiotic by a novel Bi2Sn2O7/Bi2MoO6 S-scheme heterojunction: Performance, mechanism insight and toxicity assessment. Chemical Engineering Journal, 2022, 429, 132519.	12.7	279
7	Effects of chloride ions on bleaching of azo dyes by Co2+/oxone regent: Kinetic analysis. Journal of Hazardous Materials, 2011, 190, 1083-1087.	12.4	273
8	In situ construction of WO3 nanoparticles decorated Bi2MoO6 microspheres for boosting photocatalytic degradation of refractory pollutants. Journal of Colloid and Interface Science, 2019, 556, 335-344.	9.4	219
9	Pivotal roles of MoS2 in boosting catalytic degradation of aqueous organic pollutants by Fe(II)/PMS. Chemical Engineering Journal, 2019, 375, 121989.	12.7	192
10	Peroxymonosulfate activation by phosphate anion for organics degradation in water. Chemosphere, 2014, 117, 582-585.	8.2	186
11	Facile synthesis of cerium oxide nanoparticles decorated flower-like bismuth molybdate for enhanced photocatalytic activity toward organic pollutant degradation. Journal of Colloid and Interface Science, 2018, 530, 171-178.	9.4	167
12	Synergetic Transformations of Multiple Pollutants Driven by Cr(VI)–Sulfite Reactions. Environmental Science & Technology, 2015, 49, 12363-12371.	10.0	163
13	Facile synthesis of flower-like Ag 3 VO 4 /Bi 2 WO 6 heterojunction with enhanced visible-light photocatalytic activity. Journal of Colloid and Interface Science, 2017, 501, 156-163.	9.4	152
14	Novel Photo-Sulfite System: Toward Simultaneous Transformations of Inorganic and Organic Pollutants. Environmental Science & Technology, 2013, 47, 11174-11181.	10.0	149
15	3D mesoporous α-Co(OH)2 nanosheets electrodeposited on nickel foam: A new generation of macroscopic cobalt-based hybrid for peroxymonosulfate activation. Chemical Engineering Journal, 2020, 380, 122447.	12.7	127
16	Photocatalytic degradation and chlorination of azo dye in saline wastewater: Kinetics and AOX formation. Chemical Engineering Journal, 2012, 192, 171-178.	12.7	123
17	Synergistic effect of TiO2 photocatalytic advanced oxidation processes in the treatment of refinery effluents. Chemical Engineering Journal, 2020, 391, 123488.	12.7	117
18	Synergistic effects of hybrid advanced oxidation processes (AOPs) based on hydrodynamic cavitation phenomenon – A review. Chemical Engineering Journal, 2022, 432, 134191.	12.7	117

#	Article	IF	CITATIONS
19	Simultaneous Redox Conversion of Chromium(VI) and Arsenic(III) under Acidic Conditions. Environmental Science & Technology, 2013, 47, 6486-6492.	10.0	115
20	Selective Oxidation of Arsenite by Peroxymonosulfate with High Utilization Efficiency of Oxidant. Environmental Science & Technology, 2014, 48, 3978-3985.	10.0	113
21	Insights into paracetamol degradation in aqueous solutions by ultrasound-assisted heterogeneous electro-Fenton process: Key operating parameters, mineralization and toxicity assessment. Separation and Purification Technology, 2021, 266, 118533.	7.9	113
22	Nanostructured Co3O4 grown on nickel foam: An efficient and readily recyclable 3D catalyst for heterogeneous peroxymonosulfate activation. Chemosphere, 2018, 198, 204-215.	8.2	109
23	Enhanced degradation of Tetrabromobisphenol A in water by a UV/base/persulfate system: Kinetics and intermediates. Chemical Engineering Journal, 2014, 254, 538-544.	12.7	106
24	Non-radical reactions in persulfate-based homogeneous degradation processes: A review. Chemical Engineering Journal, 2021, 421, 127818.	12.7	103
25	Transformations of chloro and nitro groups during the peroxymonosulfate-based oxidation of 4-chloro-2-nitrophenol. Chemosphere, 2015, 134, 446-451.	8.2	100
26	Sulfate radical-induced degradation of 2,4,6-trichlorophenol: A de novo formation of chlorinated compounds. Chemical Engineering Journal, 2013, 217, 169-173.	12.7	97
27	Significantly enhanced base activation of peroxymonosulfate by polyphosphates: Kinetics and mechanism. Chemosphere, 2017, 173, 529-534.	8.2	96
28	Hierarchical MnO2 nanoflowers blooming on 3D nickel foam: A novel micro-macro catalyst for peroxymonosulfate activation. Journal of Colloid and Interface Science, 2020, 571, 142-154.	9.4	94
29	Peroxymonosulfate/base process in saline wastewater treatment: The fight between alkalinity and chloride ions. Chemosphere, 2018, 199, 84-88.	8.2	93
30	Probing the radical chemistry in UV/persulfate-based saline wastewater treatment: Kinetics modeling and byproducts identification. Chemosphere, 2014, 109, 106-112.	8.2	91
31	Co3O4 nanocrystals/3D nitrogen-doped graphene aerogel: A synergistic hybrid for peroxymonosulfate activation toward the degradation of organic pollutants. Chemosphere, 2018, 210, 877-888.	8.2	81
32	In situ nitrogen functionalization of biochar via one-pot synthesis for catalytic peroxymonosulfate activation: Characteristics and performance studies. Separation and Purification Technology, 2020, 241, 116702.	7.9	81
33	Enhanced Cr(<scp>vi</scp>) removal from aqueous solutions using Ni/Fe bimetallic nanoparticles: characterization, kinetics and mechanism. RSC Advances, 2014, 4, 50699-50707.	3.6	76
34	Deciphering the degradation/chlorination mechanisms of maleic acid in the Fe(II)/peroxymonosulfate process: An often overlooked effect of chloride. Water Research, 2018, 145, 453-463.	11.3	73
35	Enhanced AOX accumulation and aquatic toxicity during 2,4,6-trichlorophenol degradation in a Co(II)/peroxymonosulfate/Clâ~ system. Chemosphere, 2016, 144, 2415-2420.	8.2	72
36	A Bimetallic Fe–Mn Oxide-Activated Oxone for In Situ Chemical Oxidation (ISCO) of Trichloroethylene in Groundwater: Efficiency, Sustained Activity, and Mechanism Investigation. Environmental Science & Technology, 2020, 54, 3714-3724.	10.0	72

#	Article	IF	CITATIONS
37	Leaching of heavy metals from Dexing copper mine tailings pond. Transactions of Nonferrous Metals Society of China, 2013, 23, 3068-3075.	4.2	66
38	Monochlorophenols degradation by UV/persulfate is immune to the presence of chloride: Illusion or reality?. Chemical Engineering Journal, 2017, 323, 124-133.	12.7	65
39	Photochemical Cycling of Iron Mediated by Dicarboxylates: Special Effect of Malonate. Environmental Science & Technology, 2010, 44, 263-268.	10.0	60
40	Concentration profiles of chlorine radicals and their significances in •OH-induced dye degradation: Kinetic modeling and reaction pathways. Chemical Engineering Journal, 2012, 209, 38-45.	12.7	60
41	A green approach towards simultaneous remediations of chromium(VI) and arsenic(III) in aqueous solution. Chemical Engineering Journal, 2015, 262, 1144-1151.	12.7	58
42	Rapid dye degradation with reactive oxidants generated by chloride-induced peroxymonosulfate activation. Environmental Science and Pollution Research, 2013, 20, 6317-6323.	5.3	56
43	Adsorptive removal of PPCPs from aqueous solution using carbon-based composites: A review. Chinese Chemical Letters, 2022, 33, 3585-3593.	9.0	53
44	EPR Evidence for Mechanistic Diversity of Cu(II)/Peroxygen Oxidation Systems by Tracing the Origin of DMPO Spin Adducts. Environmental Science & Technology, 2022, 56, 8796-8806.	10.0	52
45	The roles of polycarboxylates in Cr(VI)/sulfite reaction system: Involvement of reactive oxygen species and intramolecular electron transfer. Journal of Hazardous Materials, 2016, 304, 457-466.	12.4	49
46	Sequential reduction–oxidation for photocatalytic degradation of tetrabromobisphenol A: Kinetics and intermediates. Journal of Hazardous Materials, 2012, 241-242, 301-306.	12.4	48
47	Photochemical Coupling Reactions between Fe(III)/Fe(II), Cr(VI)/Cr(III), and Polycarboxylates: Inhibitory Effect of Cr Species. Environmental Science & Technology, 2008, 42, 7260-7266.	10.0	45
48	Effects of chloride on PMS-based pollutant degradation: A substantial discrepancy between dyes and their common decomposition intermediate (phthalic acid). Chemosphere, 2017, 187, 338-346.	8.2	45
49	Degradation of azo dye with activated peroxygens: when zero-valent iron meets chloride. RSC Advances, 2017, 7, 30941-30948.	3.6	45
50	A Novel Heterostructure of BiOI Nanosheets Anchored onto MWCNTs with Excellent Visible-Light Photocatalytic Activity. Nanomaterials, 2017, 7, 22.	4.1	45
51	Photochemical Coupling of Iron Redox Reactions and Transformation of Low-Molecular-Weight Organic Matter. Journal of Physical Chemistry Letters, 2012, 3, 2044-2051.	4.6	44
52	Is addition of reductive metals (Mo, W) a panacea for accelerating transition metals-mediated peroxymonosulfate activation?. Journal of Hazardous Materials, 2020, 386, 121877.	12.4	44
53	Arsenic(III) and iron(II) co-oxidation by oxygen and hydrogen peroxide: Divergent reactions in the presence of organic ligands. Chemosphere, 2013, 93, 1936-1941.	8.2	43
54	Comparison of UV/hydrogen peroxide and UV/peroxydisulfate processes for the degradation of humic acid in the presence of halide ions. Environmental Science and Pollution Research, 2016, 23, 4778-4785.	5.3	42

ZHAOHUI WANG

#	Article	IF	CITATIONS
55	Light-assisted decomposition of dyes over iron-bearing soil clays in the presence of H2O2. Journal of Hazardous Materials, 2009, 168, 1246-1252.	12.4	41
56	Oxidative degradation of iodinated X-ray contrast media (iomeprol and iohexol) with sulfate radical: An experimental and theoretical study. Chemical Engineering Journal, 2019, 368, 999-1012.	12.7	41
57	Degradation of reactive dyes by contact glow discharge electrolysis in the presence of Clâ^' ions: Kinetics and AOX formation. Electrochimica Acta, 2011, 58, 364-371.	5.2	40
58	Synthesis of n -type TaON microspheres decorated by p -type Ag 2 O with enhanced visible light photocatalytic activity. Molecular Catalysis, 2017, 435, 135-143.	2.0	40
59	Importance of reagent addition order in contaminant degradation in an Fe(<scp>ii</scp>)/PMS system. RSC Advances, 2016, 6, 70271-70276.	3.6	39
60	Photocatalytic Oxidation of Organic Pollutants Catalyzed by an Iron Complex at Biocompatible pH Values: Using O ₂ as Main Oxidant in a Fenton-like Reaction. Journal of Physical Chemistry C, 2011, 115, 4089-4095.	3.1	38
61	Coprecipitated arsenate inhibits thermal transformation of 2-line ferrihydrite: Implications for long-term stability of ferrihydrite. Chemosphere, 2015, 122, 88-93.	8.2	38
62	Quantitative evaluation of potential ecological risk of heavy metals in sewage sludge from three wastewater treatment plants in the main urban area of Wuxi, China. Chemistry and Ecology, 2015, 31, 235-251.	1.6	38
63	The mixed marriage of copper and carbon ring-g-C3N4 nanosheet: A visible-light-driven heterogeneous Fenton-like catalyst. Applied Surface Science, 2019, 488, 728-738.	6.1	38
64	On the kinetics of organic pollutant degradation with Co2+/peroxymonosulfate process: When ammonium meets chloride. Chemosphere, 2017, 179, 331-336.	8.2	37
65	Photochemical origin of reactive radicals and halogenated organic substances in natural waters: A review. Journal of Hazardous Materials, 2021, 401, 123884.	12.4	37
66	An often-overestimated adverse effect of halides in heat/persulfate-based degradation of wastewater contaminants. Environment International, 2019, 130, 104918.	10.0	36
67	Enabling simultaneous redox transformation of toxic chromium(VI) and arsenic(III) in aqueous media—A review. Journal of Hazardous Materials, 2021, 417, 126041.	12.4	34
68	Both degradation and AOX accumulation are significantly enhanced in UV/peroxymonosulfate/4-chlorophenol/Cl ^{â^²} system: two sides of the same coin?. RSC Advances, 2017, 7, 12318-12321.	3.6	33
69	A novel photosensitized Fenton reaction catalyzed by sandwiched iron in synthetic nontronite. RSC Advances, 2014, 4, 12958.	3.6	30
70	Highly efficient and rapid removal of arsenic(<scp>iii</scp>) from aqueous solutions by nanoscale zero-valent iron supported on a zirconium 1,4-dicarboxybenzene metal–organic framework (UiO-66) Tj ETQqO	0 0. œBT /	Ovænlock 10
71	Role of halide ions on organic pollutants degradation by peroxygens-based advanced oxidation processes: A critical review. Chemical Engineering Journal, 2022, 433, 134546.	12.7	28

⁷² Comparative study of interaction between pyrite and cysteine by thermogravimetric and electrochemical techniques. Hydrometallurgy, 2010, 101, 88-92.

4.3 27

#	Article	IF	CITATIONS
73	Current analytical methods for the determination of persulfate in aqueous solutions: A historical review. Chemical Engineering Journal, 2021, 416, 129143.	12.7	27
74	Distinct effects of oxalate versus malonate on the iron redox chemistry: Implications for the photo-Fenton reaction. Chemosphere, 2014, 103, 354-358.	8.2	26
75	On peroxymonosulfate-based treatment of saline wastewater: when phosphate and chloride co-exist. RSC Advances, 2018, 8, 13865-13870.	3.6	26
76	Transformation of endogenic and exogenic Cl/Br in peroxymonosulfate-based processes: The importance of position of Cl/Br attached to the phenolic ring. Chemical Engineering Journal, 2020, 381, 122634.	12.7	26
77	pH-dependent roles of polycarboxylates in electron transfer between Cr(VI) and weak electron donors. Chemosphere, 2018, 197, 367-374.	8.2	25
78	Chlorine incorporation into dye degradation by-product (coumarin) in UV/peroxymonosulfate process: A negative case of end-of-pipe treatment. Chemosphere, 2019, 229, 374-382.	8.2	25
79	Diverse redox chemistry of photo/ferrioxalate system. RSC Advances, 2014, 4, 44654-44658.	3.6	22
80	Accelerated oxidation of 2,4,6-trichlorophenol in Cu(II)/H2O2/Cl- system: A unique "halotolerant― Fenton-like process?. Environment International, 2019, 132, 105128.	10.0	22
81	Abiotic oxidation of arsenite in natural and engineered systems: Mechanisms and related controversies over the last two decades (1999–2020). Journal of Hazardous Materials, 2021, 414, 125488.	12.4	22
82	Resistance of alkyl chloride on chloramphenicol to oxidative degradation by sulfate radicals: Kinetics and mechanism. Chemical Engineering Journal, 2021, 415, 129041.	12.7	21
83	Adsorption behavior of glucose on pyrite surface investigated by TG, FTIR and XRD analyses. Hydrometallurgy, 2010, 102, 87-90.	4.3	20
84	Iron species in layered clay: Efficient electron shuttles for simultaneous conversion of dyes and Cr(VI). Chemosphere, 2014, 95, 643-646.	8.2	20
85	Chemical instability of graphene oxide following exposure to highly reactive radicals in advanced oxidation processes. Journal of Colloid and Interface Science, 2017, 507, 51-58.	9.4	20
86	Efficient degradation of industrial pollutants with sulfur (IV) mediated by LiCoO2 cathode powders of spent lithium ion batteries: A "treating waste with waste―strategy. Journal of Hazardous Materials, 2020, 399, 123090.	12.4	19
87	New insight into photochemical oxidation of Fe(II): The roles of Fe(III) and reactive oxygen species. Catalysis Today, 2014, 224, 244-250.	4.4	18
88	Ultrahigh-flux (>190,000†L·mâ^'2hâ^'1) separation of oil and water by a robust and durable Cu(OH)2 nanoneedles mesh with inverse wettability. Journal of Colloid and Interface Science, 2019, 555, 569-582.	9.4	18
89	Effects of exogenic chloride on oxidative degradation of chlorinated azo dye by UV-activated peroxodisulfate. Chinese Chemical Letters, 2021, 32, 2544-2550.	9.0	18
90	Performance of UV/acetylacetone process for saline dye wastewater treatment: Kinetics and mechanism. Journal of Hazardous Materials, 2021, 406, 124774.	12.4	17

#	Article	IF	CITATIONS
91	Interaction between pyrite and cysteine. Transactions of Nonferrous Metals Society of China, 2006, 16, 943-946.	4.2	16
92	Trace bromide ion impurity leads to formation of chlorobromoaromatic by-products in peroxymonosulfate-based oxidation of chlorophenols. Chemosphere, 2017, 182, 624-629.	8.2	16
93	Oxidative transformation of iron monosulfides and pyrite in estuarine sediments: Implications for trace metals mobilisation. Journal of Environmental Management, 2017, 186, 158-166.	7.8	15
94	Can electrochemical oxidation techniques really decontaminate saline dyes wastewater?. Journal of Environmental Chemical Engineering, 2015, 3, 1648-1653.	6.7	14
95	Experimental measurements of short-term adsorption of Acidithiobacillus ferrooxidans onto chalcopyrite. Transactions of Nonferrous Metals Society of China, 2012, 22, 442-446.	4.2	9
96	Interfacial electrokinetic characteristics before and after bioleaching microorganism adhesion to pyrite. Transactions of Nonferrous Metals Society of China, 2006, 16, 676-680.	4.2	8
97	Fe-catalyzed photoreduction of Cr(VI) with dicarboxylic acid (C ₂ –C ₅): divergent reaction pathways. Desalination and Water Treatment, 2015, 56, 1020-1028.	1.0	7
98	Is UV/Ce(iv) process a chloride-resistant AOPs for organic pollutants decontamination?. RSC Advances, 2016, 6, 93558-93563.	3.6	7
99	Probing the importance of planar surfaces and crystal edges for electron transfer within iron-bearing clays. RSC Advances, 2014, 4, 31476-31480.	3.6	6
100	Spent LiFePO4: An old but vigorous peroxymonosulfate activator for degradation of organic pollutants in water. Environmental Research, 2022, 214, 113780.	7.5	6
101	Bacterial oxidation activity in heap leaching. Central South University, 2004, 11, 375-379.	0.5	5
102	Multiwall Carbon Nanotubes-Modified Glassy Carbon Electrode for Square-Wave Stripping Voltammetric Determination of Aqueous Antimony (III) Ion. Advanced Materials Research, 2012, 518-523, 1571-1575.	0.3	4
103	Nanoscale in Photocatalysis. Nanomaterials, 2017, 7, 86.	4.1	3
104	Resolving the kinetic and intrinsic constraints of heat-activated peroxydisulfate oxidation of iopromide in aqueous solution. Journal of Hazardous Materials, 2020, 384, 121281.	12.4	3
105	Pivotal effects of external Fe2+ on remediation of arsenite by zero-valent iron/persulfate: Efficiencies and mechanism. Environmental Research, 2020, 189, 109922.	7.5	3
106	Spent rather than pristine LiFePO4 cathode materials can catalytically activate sulfite for organic pollutants decontamination. Chemical Engineering Journal, 2022, 446, 137123.	12.7	3
107	Response to Comment on "Synergetic Transformations of Multiple Pollutants Driven by Cr(VI)-Sulfite Reactions― Environmental Science & Technology, 2016, 50, 6109-6111.	10.0	2
108	Photodegradation mechanism of chlorophenols pollutants by TiO ₂ photocatalysis. Scientia Sinica Chimica, 2011, 41, 1286-1297.	0.4	2

#	Article	IF	CITATIONS
109	Application of N-F-Codoped TiO2 for the Photocatalytic Reduction of Cr(VI) under Visible Light Irradiation. International Conference on Bioinformatics and Biomedical Engineering: [proceedings] International Conference on Bioinformatics and Biomedical Engineering, 2010, , .	0.0	0
110	Fenton-like Degradation of Reactive Dyes Catalyzed by Biogenic Jarosite. Journal of Advanced Oxidation Technologies, 2014, 17, .	0.5	0